5.4 THE DUIRNAL CYCLE OF OCEANIC CONVECTION OVER THE SOUTH CHINA SEA DURING THE SOUTHEAST ASIAN MONSOON

Steven L. Aves and Richard H. Johnson
Colorado State University, Fort Collins, Colorado

1. INTRODUCTION

Understanding the diurnal cycle of tropical convection is essential in the complete understanding of the role of convection in climate. It is widely accepted that, over tropical oceans, deep convective activity is at a maximum in the early morning hours (Hendon and Woodberry (1993), Chen and Houze (1997)). Several recent studies have found that the diurnal cycle is modulated along coastlines and in the vicinity of large oceanic islands. Yang and Slingo (2001) found a signal of propagation in the Bay of Bengal, where systems preferentially traversed south-eastward through the bay and greatly influenced the diurnal cycle of the region. Here, a propagation signal is defined as a systematic variation of the phase of the maximum convective activity with a coherent spatial structure. Liberti et al. (2001) found a similar signal of propagation with systems forming along the New Guinea coast and generally propagating northeastward. The purpose of this paper is to characterize the diurnal cycle of convection associated with the onset and active periods of the 1998 Southeast Asian monsoon over the northern South China Sea (SCS).

2. METHODOLOGY

The data used for this study includes geometrically corrected, hourly observations of infrared brightness temperature from the Geostationary Meteorological Satellite (GMS)-5 satellite. The study area extends from 5º to 25ºN, 105º to 125ºE, and the resolution is 1/20 of a degree. The satellite data covers the time period of the South China Sea Monsoon Experiment (1 May 1998-30 June 1998) (Johnson and Ciesielski, 2002). All hours were very well sampled with the exception of 0200 UTC, which was missing about twice as many frames as other hours. Radar reflectivity and rain rate data, collected by the Australian Bureau of Meteorological Research Center (BMRC) C-POL polarimetric C-band Doppler radar, and centered on Dongsha Island (21º N, 116º E) were also used in this study.

Several techniques were utilized to examine the diurnal cycle of convection over the study region. Convective activity was assessed using satellite proxies, such as brightness temperature and deep convective activity (DCA) (Hendon and Woodberry, 1993), and radar observations, such as corrected reflectivities and rain rates. Composite analysis was performed by averaging similar hours (e.g. all 0000 UTC IR brightness temperature frames) and comparing the subsequent time series to a sinusoidal variation one day in length. Cloud and time cluster analysis was performed in a manner similar to Mapes and Houze (1993), where continuous areas of brightness temperatures lower than an arbitrary threshold value are defined as cloud clusters, and those cloud clusters that can be temporally connected by overlapping areas in adjacent satellite frames are called time clusters.

Hovmöller diagrams of IR brightness temperature (e.g. Figure 1) reveal that the most convectively active period over the northern SCS (15 May through 14 June, hereafter MYJN) can be logically subdivided into three active subperiods based on the location and duration of convective systems. 15-20 May was the first subperiod, which coincided with the onset of convection over the northern SCS. From 21-31 May (2nd subperiod), the main convective activity shifted southward into the central SCS, and from 1-10 June (3rd subperiod) the activity shifted northward back into the northern SCS. Radar data coverage fully extends over the first subperiod, but only partially covers the other two, so its analysis will be restricted to the first subperiod.

3. RESULTS

In general, the phase of the diurnal cycle of convective activity over the northern SCS did not follow the early morning maximum typically found over open tropical waters. Figure 2 shows the time series of hourly basin-wide averages of IR

Corresponding author address: Steven L. Aves, Department of Atmospheric Science, Colorado State University, Fort Collins, CO 80525; aves@atmos.colostate.edu

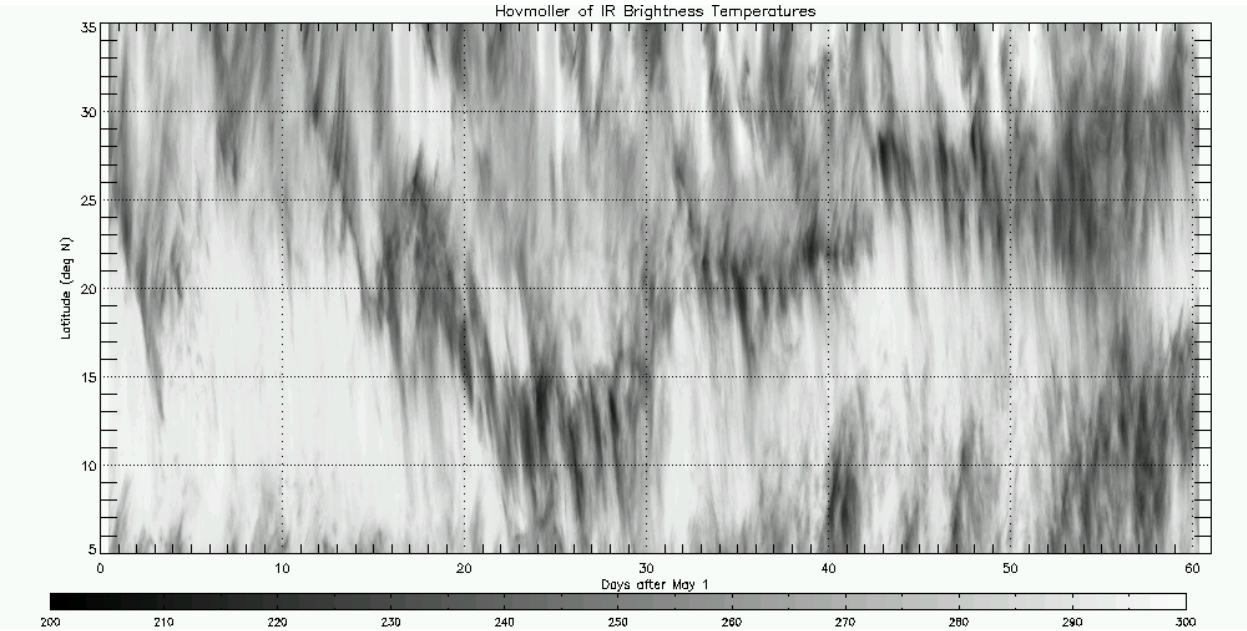

Figure 1: Hovmöller of IR brightness temperature plotted from 1 May – 30 June 1998. Values along abscissa are days after 1 May. Note the stepwise pattern of convection throughout the monsoon period, and the southward propagation of many of the individual cloud elements.

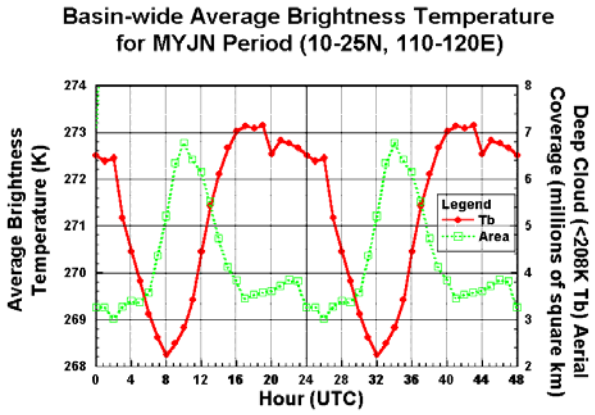

Figure 2: Time series of hourly average IR brightness temperatures for all water pixels in the northern SCS. Also shown is the hourly deep cloud aerial coverage. The time series are repeated to emphasize the periodic nature of the variations.

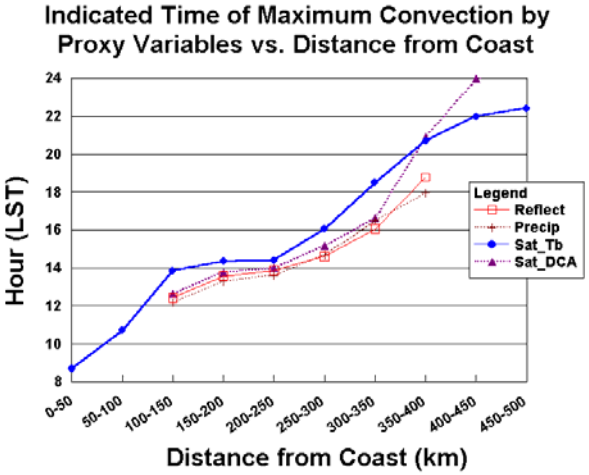

Figure 3: Indicated time of maximum convection by radar reflectivity, radar estimated precipitation, satellite brightness temperature, and deep convective activity. The data have been grouped into categories based on

brightness temperatures for water pixels only, composited on an hourly basis, and repeated to emphasize periodicity. Also shown in Figure 2 is the aerial coverage of deep convective clouds, which are defined as having IR brightness temperatures lower than 208K (Mapes and Houze, 1993). Both would indicate a maximum in convection around 0800 UTC and 1000 UTC (approximately 1600 and 1800 LST), respectively. Cloud cluster analysis shows the maximum frequency of cloud clusters over the region to be around 1000 UTC, regardless of size. This result conflicts with the findings of Chen and Houze (1997), whose study over the open tropical Pacific found an early morning maximum in the number and cumulative area of large cloud clusters.

A propagation signal, emanating from the southeastern coast of China, was evident in both satellite and radar data for both the entire MYJN period and its subperiods. A Hovmöller diagram of IR brightness temperatures, with latitude plotted against time, is shown in Figure 1. The southward

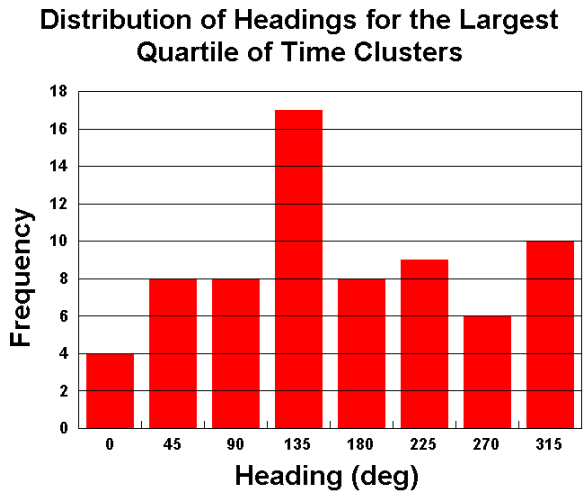

Figure 4: Direction of motion for the largest quartile of time clusters. The heading was calculated from the point of initiation to the point of dissipation.

propagation of most of the large convective clusters in the domain is easily ascertained. Figure 3 shows the signal evident in subperiod one (15-20 May). Hourly composities of IR brightness temperature, deep convective activity, corrected radar reflectivity, and radar-estimated precipitation rates were computed for each available data pixel. The pixels were then averaged according to their distance from the coast of China. These averaged time series were regressed against a sinusoidal variation one day in length, where goodness of fit was expressed as the linear correlation coefficient between the two time series. The phase of the maximum of convective activity implied by each variable is plotted in Figure 3 (maxima in DCA, reflectivity, and precipitation rates; minima in IR brightness temperature). Only the data points with significant regressed amplitudes are shown. All of the variables change phase in step, indicating a maximum of convective activity around 0800 UTC near the coast, but later in the day as distance from the coast increases. The phase speed of propagation was approximately 15 m s^{-1}. Satellite and radar observations matched well, indicating that the analysis of satellite data by itself is valid. The analysis of the other subperiods and MYJN period as a whole yields quantitatively similar results, with a propagation signal away from the China coast

Time cluster analysis of the convective systems in the region also suggests propagation generally away from the China coast. A plot of the paths of time clusters during the MYJN period reveals a preference for larger systems to move in an easterly or southeasterly fashion. Figure 4 shows this graphically by displaying the frequency of the lifetime headings of the largest quartile of time clusters. A full 25% of the time clusters moved in a southeast direction, almost double that of any other direction. Chen and Houze (1997) show that the diurnal cycle of convection is largely dependent on the life cycle of the largest cloud systems, so this preferential direction of propagation of large cloud systems over the area of interest is likely dominating the diurnal cycle.

4. ACKNOWLEDGEMENTS

This research has been supported by the National Aeronautics and Space Administration under Grant NAG5-9665. We thank Paul Ciesielski, Tom Keenan, and Michael Whimpey for their assistance.

5. REFERENCES

Chen, S. S., and R. A. Houze, 1997: Diurnal variation and life-cycle of deep convective systems over the tropical Pacific warm pool. *Quart. J. Roy. Meteorol. Soc.,* **123**, 357-388.

Hendon, H. H., and K. Woodberry, 1993: The diurnal cycle of tropical convection. *J. Geophys. Res.,* **98,** 16623-16637.

Johnson, R. H., and P. E. Ciesielski, 2002: Characteristics of the 1998 summer monsoon onset over the northern South China Sea. *J. Meteor. Soc. Japan,* **80,** 561-578.

Liberti, G. L., F. Chéruy, and M. Desbois, 2001: Land effect on the diurnal cycle of clouds over the TOGA COARE area, as observed from GMS IR data. *Mon. Wea. Rev.,* **129,** 1500-1517.

Mapes, B. E., and R. A. Houze, 1993: Cloud clusters and superclusters over the oceanic warm pool. *Mon. Wea. Rev.,* **121,** 1398-1415.

Yang, G.-Y., and J. Slingo, 2001: The diurnal cycle in the tropics. *Mon. Wea. Rev.,* **129,** 784-801